

---

# GD doesn't make the cut: Three ways that non-differentiability affects neural network training

---

Siddharth Krishna Kumar<sup>\* 1</sup>

## Abstract

This paper investigates the distinctions between gradient methods applied to non-differentiable functions (NGDMs) and classical gradient descents (GDs) designed for differentiable functions. First, we demonstrate significant differences in the convergence properties of NGDMs compared to GDs, challenging the applicability of the extensive neural network convergence literature based on  $L$  – *smoothness* to non-smooth neural networks. Next, we demonstrate the paradoxical nature of NGDM solutions for  $L_1$ -regularized problems, showing that increasing the regularization penalty leads to an increase in the  $L_1$  norm of optimal solutions in NGDMs. Consequently, we show that widely adopted  $L_1$  penalization-based techniques for network pruning do not yield expected results. Additionally, we dispel the common belief that optimization algorithms like Adam and RMSProp perform similarly in non-differentiable contexts. Finally, we explore the Edge of Stability phenomenon, indicating its inapplicability even to Lipschitz continuous convex differentiable functions, leaving its relevance to non-convex non-differentiable neural networks inconclusive. Our analysis exposes misguided interpretations of NGDMs in widely referenced papers and texts due to an overreliance on strong smoothness assumptions, emphasizing the necessity for a nuanced understanding of foundational assumptions in the analysis of these systems.

Gradient Descent (GD) and its variants (Duchi et al., 2011; Kingma & Ba, 2014; Lydia & Francis, 2019; McMahan & Streeter, 2010; Shi & Li, 2021; Tieleman et al., 2012; Zhang, 2018) have played a pivotal role in advancing image and language processing over the last two decades. These algorithms have found widespread use in neural network

<sup>\*</sup>Equal contribution <sup>1</sup>Upwork inc., San Francisco, USA. Correspondence to: Siddharth Krishna Kumar <siddharthkumar@upwork.com>.

training because they are easy to implement, highly scalable, and iteratively approach stationary points, where the loss function's gradient is zero (Bertsekas, 1997).

Despite being initially designed for differentiable loss functions, GDs are widely used to minimize the loss functions of non-differentiable neural networks. The loss functions of these non-differentiable neural networks take a special form – they are differentiable almost everywhere. Consequently, when gradient descents are applied to these non-differentiable neural networks (which we refer to as non-differentiable gradient methods or NGDMs), they seldom encounter non-differentiable points during the training process. This trait, combined with recent findings that NGDMs converge to stationary points under mild regularity conditions (Bolte & Pauwels, 2021; Davis et al., 2020), has led standard references in the field to assume that non-differentiability in neural networks is inconsequential (see Section 6.1.5 of (Stevens et al., 2020), for instance). To emphasize this point, we note that three of the most widely cited surveys on optimization methods for neural networks (Bottou et al., 2018; Le et al., 2011; Ruder, 2016) do not mention non-differentiability, even though the ReLU, arguably the most common activation function in neural networks, is non-differentiable.

Moreover, this assumption has sparked renewed interest in the dynamics of gradient descents amid complex loss landscapes ((Ahn et al., 2022b; Dauphin et al., 2014; Reddi et al., 2019) to state a few), with fewer studies explicitly addressing non-differentiability (Bertoin et al., 2021; Bolte & Pauwels, 2021; Davis et al., 2020). Additionally, it has led theoretical papers to develop results for continuously differentiable functions and then claim universality by running simulations on non-differentiable neural networks (Experiment 6 in (Ahn et al., 2022b), Section 3.1 in (Ma et al., 2022), Section 6 in (Zhang et al., 2022) to state a few).

In our paper, we challenge this assumption, demonstrating that it leads to inaccuracies in several highly referenced papers and texts regarding training dynamics in neural networks. We analyze three different aspects of the training process and make the following contributions:

- **Convergence Analysis of ReLU Networks:** We

show that the rate of convergence of NGDMs is slower than that of GDs. Our findings strongly suggest that the many claims about rate of convergence made under the assumption of  $L$ -smoothness have little bearing on the properties of NGDMs. Furthermore, we dispel the widespread belief that different NDGM variants like RMSProp and Adam largely differ only in their rates of convergence, but converge to roughly the same eventual point in the limit.

- **Solution to the LASSO problem:** We show that NGDMs, including variants like RMSProp and NDGM with momentum, do not produce sparse solutions for the LASSO problem, even for the simplest case of the  $L_1$  penalized linear model, and exhibit different behaviors, contrary to prevalent wisdom. Moreover, NGDMs can yield counterintuitive results, such as producing a solution with a larger  $L_1$  norm with a larger LASSO penalty.
- **The Edge of Stability:** We demonstrate that the edge of stability conjecture does not hold, even for gradient descents on all convex differentiable neural networks. Furthermore, we provide a counter-example to the claim made in (Ma et al., 2022) that subquadratic behavior around the local minimum is responsible for the Edge of Stability phenomenon.

In a broader context, our analysis emphasizes the critical role the assumptions we make play on our understanding of these complex systems. For NGDMs in particular, our results suggest a need to treat GDs and NGDMs as distinct systems with different dynamics, challenging the common assumption of their similarity.

## 1. Preliminaries

In the three sections that follow, we show how disregarding the non-differentiability of the loss function severely limits our understanding of different aspects of training dynamics. Each of these sections is largely self-contained, complete with a literature review, problem setup, and analysis. Throughout this paper, experiments involving deep networks consistently employ convolutional neural network (CNN) architectures akin to VGG16 (Simonyan & Zisserman, 2014). This choice is motivated by the architecture's widespread usage in the papers referenced throughout our discussions. Our experiments have relatively low computational costs, with the most expensive run completing within 2 hours on a single GPU. The present section addresses background and terminology that is pertinent to all the subsequent sections.

**NDGM v/s GD:** The crux of our analyses lies in the structural differences between GDs and NDGMs. For a contin-

uously differentiable loss function,  $f(\beta)$ , the well-studied GD sequence (Bertsekas, 1997; Boyd et al., 2004) is described by the recursion

$$\beta_{t+1} = \beta_t - \alpha \nabla f(\beta_t), \quad (1)$$

where  $\alpha$  is the learning rate, and  $\beta_0$  is a randomly initialized starting point.

For a continuous non-differentiable loss function,  $g(\beta)$ , the NDGM recursion is given by

$$\tilde{\beta}_{t+1} = \tilde{\beta}_t - \alpha \tilde{\nabla} g(\tilde{\beta}_t), \quad (2)$$

where  $\tilde{\nabla} g(\tilde{\beta}_t) = \nabla g(\tilde{\beta}_t)$  if the gradient exists at  $\tilde{\beta}_t$ , else it is a heuristic measure<sup>1</sup>. The deep learning literature widely assumes that the dynamics described by the recursions in (1) and (2) are nearly the same.

**Convex non-differentiable loss functions:** In this paper, we show the problems with this assumption using a variety of convex loss functions. The majority of our analysis is performed on the penalized single layer neural network regression problem with a non-positive response vector, which (Kumar, 2023) has shown to be convex with the all-zeros vector as its unique global minimizer. The loss function for this problem is given by

$$L_1(\beta; \mathbf{Z}, \mathbf{y}, \lambda_1, \lambda_2) = \|\mathbf{y} - \max(0, \mathbf{Z}\beta)\|^2 + \lambda_1 \|\beta\|_1 + \lambda_2 \|\beta\|_2^2, \quad (3)$$

where  $\beta$  is a  $P \times 1$  parameter vector,  $\mathbf{Z}$  is an  $N \times P$  data matrix whose  $i^{th}$  column is given by  $z_i$ ,  $\mathbf{y}$  is a  $N \times 1$  non-positive response vector,  $\lambda_1 \geq 0$  is the LASSO penalty,  $\lambda_2 \geq 0$  is the ridge penalty, and  $\lambda_1 + \lambda_2 > 0$ . Throughout this paper, we denote the learning rate by  $\alpha$ , and the  $i^{th}$  entry in the parameter vector after  $k$  iterations as  $\beta_k[i]$ , with  $0 \leq i \leq P - 1$ .

**The subgradient method:** Our analysis heavily relies on the observation that for a convex non-differentiable loss functions, the NDGM recursion described in (2) effectively implements the subgradient method (Bertsekas, 1997; Shor, 2012). The theoretical properties of this method are well studied in the optimization literature, with a concise overview of key findings available in the lecture notes of (Boyd et al., 2003) and (Tibshirani, 2015). The subgradient method and GD recursions have different properties, and these differences play a key role in our subsequent discussions. We reference the relevant portions from the lecture notes as they arise.

<sup>1</sup><https://rb.gy/g74av>

**Constant, diminishing, and reducing step sizes:** Our formulations in equations (1) and (2) employ a constant learning rate. This choice bears some explaining, for which we first recall some definitions from the optimization literature (see Chapter 1 of (Bertsekas, 1997) for details). In the GD literature, the training regimen described in equation (1) is called a constant step-size regime. In this regime, the GD is initialized using some randomized approach, and iterated with a constant learning rate until the loss stops decreasing. Although constant step-size GDs approach the stationary point, they rarely converge to it unless the loss function possesses desirable properties like  $L$ -smoothness (Proposition 1.2.3 in (Bertsekas, 1997)). To ensure provable convergence to the stationary point in more general settings, studies often adopt the diminishing step-size regime. This regime is characterized by the iteration

$$\beta_{t+1} = \beta_t - \alpha_t \nabla f(\beta_t), \quad (4)$$

where  $\lim_{t \rightarrow \infty} \alpha_t = 0$ , and  $\sum_t \alpha_t \rightarrow \infty$ . Convergence results in this regime are derived under ideal conditions, and provide guarantees that the recursion will reach the stationary point at least in the theoretical limit. In practice, diminishing step-size GDs are implemented with a stopping criteria which determines when the solution produced by the GD is good enough to end training. The combination of the diminishing step-size regime and stopping criteria commonly used in the neural network literature is what we term the “reducing” step-size regime.

In this regime, training unfolds as follows: commencing with a weight of  $\beta_0$ , GD is run for some  $N_0$  iterations with a learning rate of  $\alpha_0$ , followed by  $N_1$  iterations with a reduced learning rate of  $\alpha_1 < \alpha_0$ , and so on, until the engineer is satisfied with the solution. In the reducing step-size regime, training involves chaining together a finite number (say  $T$ ) of constant step-size GD runs, with the  $(i+1)^{th}$  run having an initialization of  $\beta_u$  and a learning rate of  $\alpha_i$ , where  $u = \sum_{j=0}^{i-1} N_j$ . While the theoretical guarantees of the diminishing step-size regime may not be realized, the limiting dynamics of the sequence in this regime are exactly those of a constant step-size GD, with learning rates and weight initializations chosen corresponding to the values at the beginning of the  $T^{th}$  run. Accordingly, we exclusively study the constant step-size problem, assuming appropriate weights and learning rates have been chosen.

## 2. NDGM and convergence analysis

Recent theoretical work by (Davis et al., 2020) has shown that in the diminishing step-size regime, NDGMs converge to a local optimal solution in the theoretical limit under fairly general conditions. Unfortunately, the conditions of the diminishing step size regime are rarely satisfied in prac-

tice. To illustrate this point, consider the Assumption A.3 in (Davis et al., 2020), which requires that in the diminishing step size regime, the sum of the learning rates should diverge. As was previously stated, this is a standard assumption even in the theoretical convergence analysis of GDs. However, the prevalent step-size reduction we observed in most training scripts involves decaying the learning rate by a constant multiplicative factor at predefined intervals (StepLR in PyTorch<sup>2</sup>). With this decay scheme, the learning rates form a convergent geometric series, thus violating the assumption.

For the differentiable case, we know that even when the learning rates form a convergent geometric series, the GD sequence will come within some vicinity of the optimal solution. Therefore, the question arises if the same holds true for NDGM sequences. More precisely, can we state that the dynamics of NDGM and GD sequences are identical?

**NDGM and GD dynamics are not identical:** The dynamics of the two sequences are not identical, and we demonstrate this by arriving at a contradiction. Suppose the sequence  $\{\beta_k\}_{k=0}^{\infty}$  obtained by running NDGM on  $L_2(\beta; \mathbf{Z}_1, \mathbf{q}_1) = L_1(\beta; \mathbf{Z}_1, \mathbf{q}_1, 0, 0.01)$  has the same properties as a GD sequence. Then, the entire NDGM sequence can be characterized using the “Capture Theorem” as described below

**Proposition 2.1.** *Let  $x_{k+1} = x_k - \alpha \nabla f(x_k)$  be a sequence generated by running GD on a continuously differentiable function,  $f(x)$  such that  $f(x_{k+1}) \leq f(x_k)$ . If  $x^*$  is an isolated local minimum of  $f(x)$  in a unit ball around  $x^*$ , and  $\|x_0 - x^*\| < 1$ , then  $\|x_k - x^*\| < 1$  for all  $k > 0$ .*

*Proof.* Result follows by using  $\bar{\epsilon} = 1$  in Proposition 1.2.5 of (Bertsekas, 1997).  $\square$

Therefore, if  $\|\beta_0\|_{\infty} < 1$ , and  $L_2(\beta_{k+1}; \mathbf{Z}_1, \mathbf{q}_1) \leq L_2(\beta_k; \mathbf{Z}_1, \mathbf{q}_1)$  for all  $k \geq 0$ , then we expect  $\|\beta_k\|_{\infty} < 1$  for all  $k \geq 0$ . To validate this claim, we first generate a  $20 \times 500$  matrix  $\mathbf{Z}_1$  with entries uniformly sampled on  $[-1, 1]$ . Next, we generate a  $20 \times 1$  vector  $\mathbf{q}_1$  with entries uniformly sampled on  $[-1, 0]$ . Finally, we generate the sequence  $\{\beta_t\}_{t=0}^{\infty}$ , by running NDGM on  $L_2(\beta; \mathbf{Z}_1, \mathbf{q}_1)$  with the entries in  $\beta_0$  uniformly sampled on  $[-1, 1]$ . As seen in Figure 1, although the loss function is a monotone decreasing function of the iteration number, the infinity norm of the NDGM sequence eventually takes values greater than 1, hence establishing the contradiction. The non-capturing described in Figure 1 is to be expected; as stated in Section 1 of (Boyd et al., 2003), “Unlike the ordinary gradient method, the subgradient method is not a descent method; the function value can (and often does) increase”.

<sup>2</sup><https://rb.gy/pub4s>

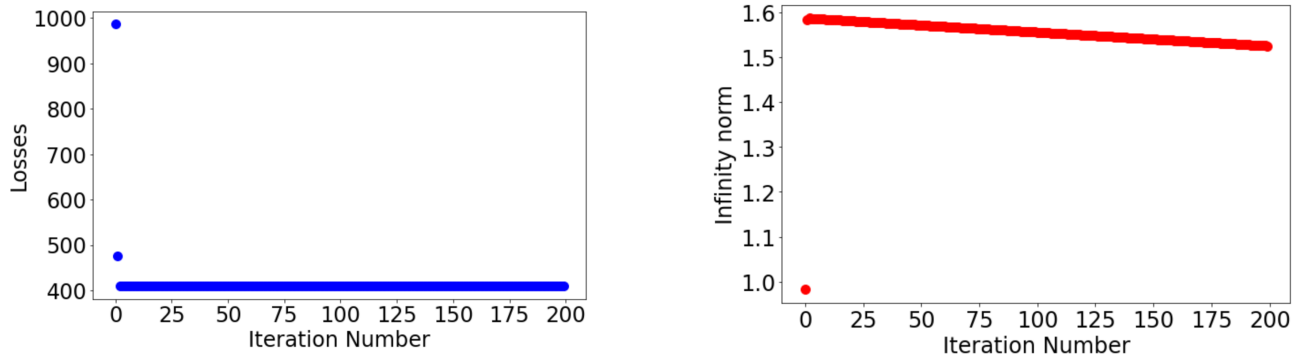


Figure 1. Plot of the loss function ( $L_2(\beta_k; \mathbf{Z}_1, \mathbf{q}_1)$ ), and infinity norm ( $\|\beta_k\|_\infty$ ) of the parameter vector as a function of the iteration number ( $k$ ). Although the loss function is monotone decreasing, the infinity norm of the weights does not “capture”, hence demonstrating that the dynamics of NDGM and GD are not identical

**Convergence analysis and  $L$ -smoothness:** Given that the dynamics of GDs and NDGMs differ, the question arises what assumptions are appropriate for the study of convergence analysis in neural network training. Majority of the analyses in the literature ((Bottou et al., 2018; Zhang et al., 2022; Défossez et al., 2020; You et al., 2019) to state a few) assume that the loss function,  $f(\beta)$  is continuously differentiable, and is  $L$ -smooth, i.e., there exists a constant  $L$ , such that

$$\|\nabla f(x) - \nabla f(y)\| \leq L\|x - y\| \quad (5)$$

for all  $x, y$  in the domain of  $f$ . However, this assumption breaks down for non-differentiable functions, where the gradient does not even exist at various points in the domain. This raises the question if the assumption can be salvaged by confining its validity to a local context around the local optimal solution.

Unfortunately, even this cannot be done; as stated in (Lau- rent & Brecht, 2018), “local minima of ReLU networks are generically nondifferentiable. They cannot be waved away as a technicality, so any study of the loss surface of such network must invoke nonsmooth analysis”. Moreover, assuming that the loss function is  $L$ -smooth grossly over-estimates the speed of convergence of NDGMs. To illustrate this, consider that in order to achieve an error level of  $\epsilon$ , GD applied to an  $L$ -smooth convex loss function,  $f$ , would require  $O(1/\epsilon)$  steps for convergence. In contrast, NDGM applied to a convex non-differentiable loss function,  $g$ , satisfying the Lipschitz condition

$$\|g(x) - g(y)\| \leq L\|x - y\| \quad (6)$$

would take  $O(1/\epsilon^2)$  steps (see Section 7.1.3 of (Tibshirani, 2015) for the result, and a visual illustration of how much slower  $O(1/\epsilon^2)$  is than  $O(1/\epsilon)$ ). Thus, it is likely that the vast literature on the convergence analysis of GDs for loss

functions satisfying (5) have little bearing on the dynamics of convergence in modern non-smooth neural networks. More generally, we expect the speed of convergence for smooth neural networks to be faster than that of non-smooth neural networks.

**Experiments with NDGM convergence:** We conduct two sets of experiments on CNNs of varying depths to validate our intuition in a more general context (see the Appendix A for architecture details). In each set, we perform two identical simulations for every network, with the only difference being the choice of activation function: one simulation uses the non-smooth ReLU activation function, while the other uses the smooth and asymptotically equivalent GELU activation function (Hendrycks & Gimpel, 2016). The first set of experiments excludes batch normalization, while the second includes it.

Figure 2 shows that without batch normalization, the gap in convergence speeds between smooth and non-smooth networks widens as network depth increases, aligning with our expectations. This trend is further substantiated by (Hendrycks & Gimpel, 2016), who demonstrate accelerated convergence in GELU networks compared to ReLU networks across diverse architectures and datasets (see Figures 2 through 7 in their paper). However, with batch normalization, the difference between ReLU and GELU training curves becomes indistinguishable, emphasizing its importance in the training process. We conclude that the choice of activation function is the primary factor contributing to the difference in convergence speeds between ReLU and GELU curves with increasing depth, as no other principled reason appears evident.

**$L$ -smoothness and the geometry of ReLU networks:** As stated in (Bottou, 2010), the assumption of  $L$ -smoothness ensures that the gradient of the loss function does not change

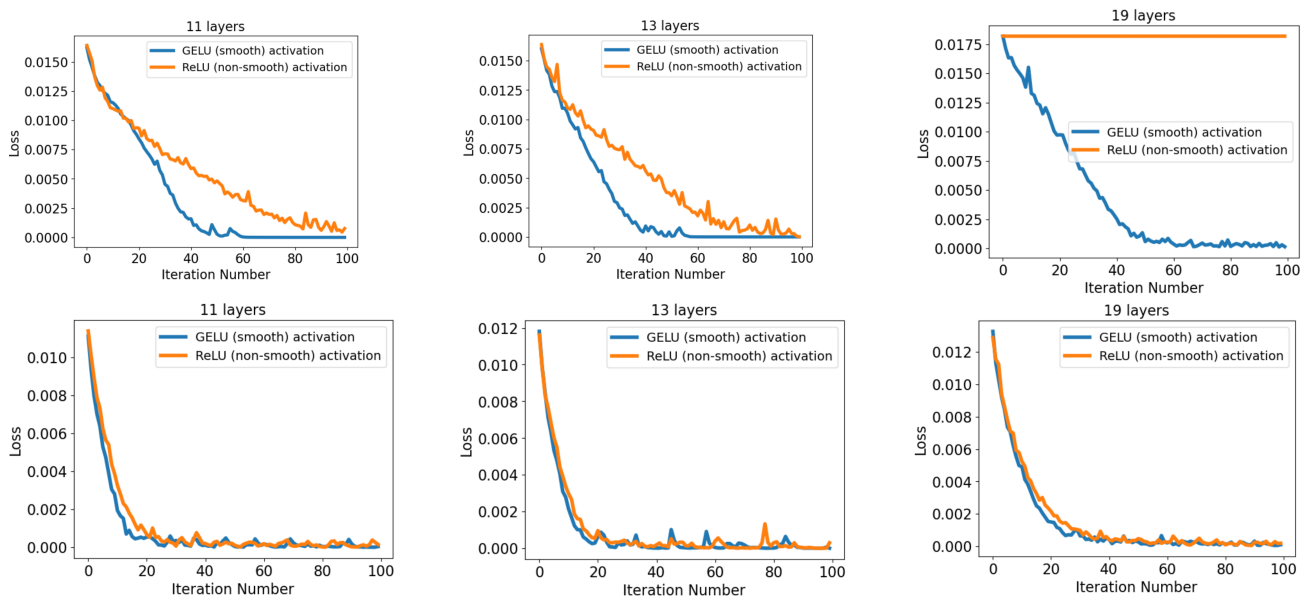


Figure 2. Training curves comparing smooth and non-smooth CNNs (from left to right) of depth 11, 13, and 19, respectively. The top row shows validation losses without batch normalization, while the bottom row includes batch normalization.

too rapidly with respect to the parameter vector. However, this assumption which does not hold for ReLU networks. To illustrate this, consider the 1-D case with  $q(x) = \max(0, x)$ . In this case,  $\lim_{h \rightarrow 0^+} (1/2h)(\nabla q(h) - \nabla q(-h)) = \infty$ , indicating that the gradient changes arbitrarily quickly at the origin. This observation necessitates the use of non-smooth analysis for studying the loss functions of ReLU networks, as detailed in (Laurent & Brecht, 2018). The key intuition about non-differentiable functions is that they have kinks corresponding to non-differentiable points, and local minima frequently lie at these kinks. As a result, gradient descents which rely on smoothness assumptions cannot access these points of interest. This realization serves as one of the primary motivations for the development and application of second-order cone programs for convex non-smooth problems (Boyd et al., 2004)<sup>3</sup>. The inability of gradient descent methods to effectively maneuver non-smooth functions and the associated pathologies form a recurring theme throughout the remaining sections of this paper. In a subsequent section on the Edge of Stability, we show that insights based on the assumption of  $L$ -smoothness are not universally applicable even across all Lipschitz continuous, convex, differentiable neural networks.  $L$ -smoothness is one of the strongest assumptions after convexity, guaranteeing the existence and boundedness of the first and second derivatives—criteria unmet by most loss functions in neural network literature.

<sup>3</sup>See 26:30 to 29:00 in <https://rb.gy/ab0aeh>

**Limitations of our work:** A common limitation in the current and subsequent sections is that we do not analyze the dynamics of the neural network training process as it is often conducted in practice. This is necessitated by the fact that neural networks often involve non-differentiable layers like dropout and max pooling, which are beyond the scope of our study. We do not reiterate this limitation in every subsequent section.

**The way forward:** In this section, we show that NDGMs are slower to converge than GDs. Fortunately, most recent explorations into image and language models primarily leverage the transformer architecture (Vaswani et al., 2017) with the differentiable GELU activation function (Hendrycks & Gimpel, 2016). As a consequence, future iterations of neural networks may predominantly employ pure GDs. Therefore, it is crucial for the research community to establish a consensus on a set of assumptions that accurately represent these complex systems before meaningful progress can be achieved.

### 3. NDGM and the LASSO penalty

Zero weights are crucial for model compression (Blalock et al., 2020; Han et al., 2015a;b; Li et al., 2016), and inducing sparsity by penalizing the  $L_1$  norm of model weights is a common approach. While the statistics literature employs specialized algorithms for problems involving penalized  $L_1$  norms (Efron et al., 2004; Friedman et al., 2008; Mazumder & Hastie, 2012; Tibshirani, 1996; Tibshirani et al., 2005;

Zou & Hastie, 2005), neural networks often use the penalized  $L_1$  norm with arbitrary non-convex functions, assuming that NDGM results in a near-sparse optimal solution (Bengio, 2012; Goodfellow et al., 2016b; Scardapane et al., 2017). This expectation is not always met, as evidenced by user struggles in PyTorch forums<sup>4,5,6</sup>. Given the LASSO's critical applications (Ghosh et al., 2021; Li et al., 2011; Li & Sillanpää, 2012; Ogutu et al., 2012), understanding the reliability of the NDGM solution for the LASSO problem is essential.

**NDGM solutions for the LASSO problem are not reliable:** We show that NDGM produces unreliable solutions even for the simple case of the LASSO penalized linear model. In particular, we show that increasing the LASSO penalty can result in a NDGM solution with a larger  $L_1$  norm, completely defeating the purpose of the penalty. We first analytically demonstrate the unreliability for the simplest LASSO problem,

$$L_3(\beta) = L_1(\beta; 0, 0, \lambda_1, 0) = \lambda_1 \|\beta\|_1, \quad (7)$$

with  $\lambda_1 > 0$ , and then demonstrate the same issues for the general LASSO problem through simulations. We begin by showing that for any non-zero learning rate,  $\alpha$ , the NDGM sequence for (7) will be non-sparse with probability 1.

**Proposition 3.1.** *Let  $\{\beta_t\}_{t=0}^\infty$  denote the sequence generated by running NDGM on (7), with a constant learning rate,  $\alpha$ , and the entries in  $\beta_0$  being uniformly sampled from  $[-1, 1]$ . Then  $\beta_k$  will have all non-zero entries with probability 1 for all  $k > 0$ . Furthermore, there exists an integer  $N_0$ , such that for every  $N \geq N_0$ , we can write*

$$\beta_{n_k+m}[k] = \begin{cases} \gamma_k - \alpha\lambda_1 & \text{if } m \text{ is odd} \\ \gamma_k & \text{if } m \text{ is even,} \end{cases} \quad (8)$$

where  $\gamma_k \in (0, \alpha\lambda_1)$  for all  $0 \leq k \leq P - 1$ .

*Proof.* See Appendix B for details  $\square$

Equation (8) suggests that with the same learning rate and initialization, a larger  $\lambda_1$  can lead to a NDGM solution with a larger  $L_1$  norm, defeating the purpose of the LASSO penalty. To illustrate this, we note that in the 2D case, with weights initialized as  $\beta_0 = [0.5053, 0.5053]$ ,  $\alpha = 0.01$ , and  $\lambda_1 = 1$ , the NDGM sequence oscillates between  $[0.0053, 0.0053]$  and  $[-0.0047, -0.0047]$ . However, with  $\lambda_1 = 100$ , and the same values of  $\beta_0$  and  $\alpha$ , the solution oscillates between  $[0.5053, 0.5053]$  and  $[-0.4947, -0.4947]$ . Therefore at convergence, the  $L_1$  norm is at most 0.0106

for  $\lambda_1 = 1$ , but at least 0.9894 for  $\lambda_1 = 100$ . Furthermore, reducing the step-size to  $\alpha = 0.001$  after apparent convergence does not resolve this paradox. With  $\lambda_1 = 1$ , the sequence oscillates between  $[0.0003, 0.0003]$  and  $[-0.0007, -0.0007]$ , while with  $\lambda_1 = 100$ , it oscillates between  $[0.0053, 0.0053]$  and  $[-0.0947, -0.0947]$ . Appendix C shows that this paradox holds for NDGM solutions of the standard  $L_1$  regularized linear problem.

**The subgradient method and step-size choices:** The counter-intuitive behavior seen in the example above can be explained using the subgradient method. Since the loss function described in equation (7) is Lipschitz continuous (equation (6)) with  $L = \lambda_1$ , we have from (Boyd et al., 2003) (Section 2 on the Constant Step Size) that

$$\lim_{k \rightarrow \infty} \|\beta_k\|_1 < \alpha\lambda_1. \quad (9)$$

Therefore, for the same value of  $\alpha$ , the larger value of  $\lambda_1$  will result in a larger error in estimation, which is precisely what we are seeing above. This illustration also highlights the contrast between the diminishing and reducing step size regimes outlined in the preliminaries. Under the diminishing step-size regime,  $\alpha \rightarrow 0$  in the theoretical limit, and therefore, Proposition 3.1 guarantees that the optimal solution for (7) will be 0 for all  $\lambda_1 > 0$ . On the other hand, in the reducing step-size regime,  $\alpha > 0$  at the end of training, and therefore, the error in estimation becomes a critical determinant of the optimal value.

**Connections to other NDGM variants:** Conventional wisdom in deep learning theory suggests that different NDGM variants, such as NDGM with momentum and RMSProp, converge at varying rates but eventually reach similar near-optimal values (Figure 8.5 of (Goodfellow et al., 2016a), slides 64 onwards in <https://rb.gy/ojzpgm7>). However, we prove in Appendices D and E that these claims are incorrect even for the toy LASSO problem described in (7). Furthermore, our analysis reveals two interesting facts. First, that the RMSProp sequence for (7) is agnostic of the value of  $\lambda_1$  used in the analysis. Second, there is a phase transition between the RMSProp and vanilla NDGM training curves characterized by a change in the relative behavior of the training curves of the two algorithms as  $\lambda_1$  is increased from a value which is much smaller than 1 to a value much larger than 1, which cannot be explained without accounting for the non-differentiability of the  $L_1$  regularizer. These findings highlight the importance of incorporating the non-differentiability of regularizers like the  $L_1$  norm when analyzing the behavior of NDGM variants. Failing to account for non-differentiability results in an in-

<sup>4</sup><https://rb.gy/kh0qr>

<sup>5</sup><https://rb.gy/2vsry>

<sup>6</sup><https://rb.gy/6dfli>

<sup>7</sup>These slides are from one of the most widely used courses for self teaching; see 1:01:00 - 1:03:00 of <https://rb.gy/kaj976> where this precise point is made

complete understanding of the optimization dynamics. Consequently, it remains unclear how the convergence analysis of algorithms like Adam and RMSProp for differentiable loss functions, as often performed in studies such as (Reddi et al., 2019; Défossez et al., 2020; Zhang et al., 2022), relates to the dynamics of these algorithms' convergence in non-differentiable settings involving regularizers like the  $L_1$  norm or activation functions like the ReLU.

**Experiments with deep networks:** In their seminal work on network pruning, (Han et al., 2015b) propose using  $L_1$  regularization to encourage weights to approach 0, facilitating the pruning process. This approach is widely adopted in the literature (Wen et al., 2016; Xiao et al., 2019; Yang et al., 2019) and industry<sup>8</sup>. To challenge this suggestion's general applicability, we conduct two sets of experiments finetuning a pre-trained VGG16 model on CIFAR-10 using  $L_1$  penalized cross-entropy loss with a constant learning rate of  $\alpha = 0.003$  for 200 epochs. We use  $\lambda_1 = 0.0002$  in the first set and  $\lambda_1 = 2$  in the second, running three parallel trials within each set using RMSProp, SGD, and Adam. At the end of our runs, we make two key observations (Figure F.1): 1) The  $L_1$  norms at convergence differ vastly across the three variants, and 2) for SGD and Adam, larger values of  $\lambda_1$  result in a larger  $L_1$  norm at convergence. These findings suggest that the relationship between  $L_1$  regularization and prunable parameters may not be as straightforward as previously thought. Indeed, our results show that a larger  $\lambda_1$  does not necessarily correspond to more prunable parameters (Table 1): with  $\lambda_1 = 2$ , less than 0.2% of the parameters at convergence with vanilla NDGM have absolute value less than  $10^{-5}$ , but with  $\lambda_1 = 0.002$ , 99.98% do.

**Soft-thresholding and ISTA:** The observation that higher  $\lambda_1$  values do not yield more prunable parameters indicates that while soft thresholding produces sparse solutions for NDGMs, it does not find optimal solutions. This issue extends beyond NDGM to general neural network problems, where any soft thresholding solution yields sparsity but not optimality. The root cause is that soft thresholding implicitly solves a generalized ISTA problem (Chen et al., 2023), which assumes the loss function is  $L$ -smooth (point 1, Section 3.2 of (Chen et al., 2023)) - an assumption that fails to capture the non-convex and non-differentiable dynamics in general neural network settings, as discussed previously. Consequently, applying the generalized ISTA formulation relying on  $L$ -smoothness to neural networks necessarily leads to suboptimal solutions.

**NDGM and the way forward with sparsity:** While NDGMs do not inherently generate sparse solutions, itera-

<sup>8</sup>See the recommendation of the regularizer in the Training config section of <https://rb.gy/20y13m> and <https://rb.gy/i1sb6s>

tive methods have been developed for  $L_1$  regularized problems (Ma et al., 2019; Siegel et al., 2020). The realization that NDGMs lack this capability predates the widespread adoption of deep learning (Xiao, 2009). Despite this, a misconception persists in the deep learning literature, suggesting that such algorithms yield sparse solutions comparable to those from traditional machine learning frameworks like glmnet (Friedman et al., 2021) or scikit-learn (Kramer & Kramer, 2016). However, there is a fundamental disparity between these frameworks: glmnet focuses on a narrow set of problems, guaranteeing optimality, while PyTorch (Paszke et al., 2017) provides flexibility in model creation, but lacks similar guarantees. Attaining a solution at a non-differentiable point is challenging, emphasizing the importance of exploring related studies and tools rather than relying on simplistic implementations when precision is crucial.

Proposition 3.1 shows that the NDGM sequence for the non-differentiable, Lipschitz continuous, convex loss function described in (7) will not diverge to  $\infty$  for any finite value of  $\alpha$ . This is a special case of unstable convergence, a topic we cover in greater detail in the next section.

## 4. NDGM and the Edge of Stability

In recent years, there has been a growing interest on the topic of "unstable convergence". The literature on the subject (Ahn et al., 2022b;a; Arora et al., 2022; Chen & Bruna, 2022; Cohen et al., 2021; Li et al., 2022) is motivated by the finding that unlike convex quadratic forms, gradient descent on neural networks do not diverge to  $\infty$  even when the learning rate is greater than  $\alpha^* = 2/\eta$ , where  $\eta$  is the dominant eigenvalue of the loss function's Hessian. Instead, the loss function has been empirically demonstrated to converge "unstably", reducing non-monotonically on the long run.  $\alpha = \alpha^*$  is referred to in the literature as the "Edge of Stability", since it separates regions of "stable convergence" ( $\alpha < \alpha^*$ ) from regions of "unstable convergence"<sup>9</sup> ( $\alpha > \alpha^*$ ). The derivation of the Edge of Stability condition assumes that the loss function,  $f$ , is  $L$ -smooth (see equation (5)).

It is conjectured that neural networks demonstrate unstable convergence because the phenomenon is inconsistent with widespread presumptions in the field of optimization (Cohen et al., 2021; Ahn et al., 2024). This conjecture is incorrect for Lipschitz continuous, differentiable, convex functions satisfying (6) as shown in the proposition below.

<sup>9</sup>We define unstable convergence to mean "non-divergence to  $\infty$ ". Our definition is adapted from Definition 1.1 of (Arora et al., 2022). However, we deviate from their definition due to its dependence on the existence of the Hessian at all points between the current and next iterate, a condition that need not be satisfied in non-smooth neural networks.

**Proposition 4.1.** *All convex non-smooth loss functions having bounded subgradients, or satisfying equation (6) will show unstable convergence.*

*Proof.* Note that any loss function satisfying (6) has subgradients bounded above by  $L$ . Additionally, as outlined in Section 1 of Boyd et al. (2003), the deductions derived from the subgradient method hold equivalently for differentiable functions. This equivalence arises from the fact that the only admissible value for the subgradient of a differentiable convex function at any given point is, indeed, its gradient. Accordingly, using the convergence properties of the subgradient methods with constant step sizes from Section 2 of Boyd et al. (2003), we have that  $\lim_{k \rightarrow \infty} f(x_k) - f^* \leq \alpha L^2 < \infty$ , hence the result.  $\square$

The toy LASSO problem studied in (7), for which we analytically demonstrated unstable convergence in the previous section, is an example of a non-differentiable convex loss function satisfying Proposition 4.1. An example of a differentiable non-smooth convex function satisfying Proposition 4.1 is the Huber loss function, which finds use in many state of the art object detection models (Girshick, 2015; Liu et al., 2016; Ren et al., 2015). The Huber loss function is non-smooth because it is once but not twice differentiable. For a regression problem involving an arbitrary  $50 \times 1$  response vector,  $\mathbf{y} = [y_1, y_2 \dots y_N]^T$ , and an arbitrary  $50 \times 200$  data matrix,  $\mathbf{Z}$ , the Huber loss function is defined as

$$L_7(\beta) = \frac{1}{N} \sum l(i), \quad \text{where}$$

$$l(i) = \begin{cases} \frac{1}{2}(y_i - z_i^T \beta)^2 & \text{if } |(y_i - z_i^T \beta)| < 1 \\ (|y_i - z_i^T \beta| - \frac{1}{2}) & \text{otherwise} \end{cases} \quad (10)$$

where  $z_i$  is the  $i^{\text{th}}$  column of  $\mathbf{Z}$ . Figure 3 shows that the NDGM sequence for (10) does not diverge toward  $\infty$ , even with a high learning rate, such as  $\alpha = 10$ , which aligns with our expectations. Proposition 4.1 suggest that it is unclear and the examples that follow show that the common approach of extrapolating results developed for  $L$ -smooth loss functions to the non-smooth or non-differentiable case is problematic. To emphasize this point, we provide an example of such an extrapolation in the literature which breaks down in the non-smooth case.

**Subquadratic losses and unstable convergence:** In section 3.1 of (Ma et al., 2022), the authors use second-order finite differences to analyze the curvature of VGG16 and ResNet near the local minimum, concluding that subquadratic growth explains the edge of stability phenomenon. However, their analysis is flawed because ReLU networks

have generically non-differentiable local minima (Laurent & Brecht, 2018), where their approximation breaks down.

The Huber loss function described in equation (10) challenges their statement's broad applicability. This overparameterized convex function has a global minimum of 0, exhibiting quadratic growth nearby. (Ma et al., 2022)'s result suggests stable convergence, but Proposition 4 guarantees unstable convergence (Figure 3). The discrepancy arises because the Huber loss function lacks the twice differentiability required by Definition 4.1 in (Ma et al., 2022). In contrast,  $L$ -smooth functions, which are twice differentiable by definition, exhibit subquadratic growth near their local minimum during unstable convergence. This example highlights the challenges of extending results developed under strong assumptions like  $L$ -smoothness to the general case.

**The way forward:** We demonstrate that our understanding of the Edge of Stability will be incomplete until we more precisely quantify conditions under which we expect it to occur. Furthermore, considering ReLU networks' non-differentiable minima, without further research into NDGM behavior around non-differentiable points our grasp of training dynamics lacks completeness. Consequently, we propose employing the convex non-differentiable single-layer neural network presented in (Kumar, 2023) as the toy problem for theory development. Studying this neural network offers several advantages: 1) its convex nature renders it more amenable to analysis compared to non-convex functions, 2) we possess analytical knowledge of the global optimum, and 3) the global optimum exists at a point of non-differentiability—the setup which is particularly relevant to ReLU networks.

## 5. Conclusion

In this paper, we highlight how non-differentiability alters training dynamics across three domains: convergence analysis, the LASSO problem, and the Edge of Stability. In each case, we show that problems arise because of incorrect assumptions made about the contour of the loss surface. Our results suggest the critical need to reach consensus on a set of assumptions which can be made about the loss surface before progress can be made.

## 6. Acknowledgements

We would like to thank Wenyun Zuo, Boris Ginsburg, and several anonymous reviewers for inputs on earlier drafts of this paper. We would also like to thank Shripad Tuljapurkar and Marc Feldman for how to best stare at dynamical systems.

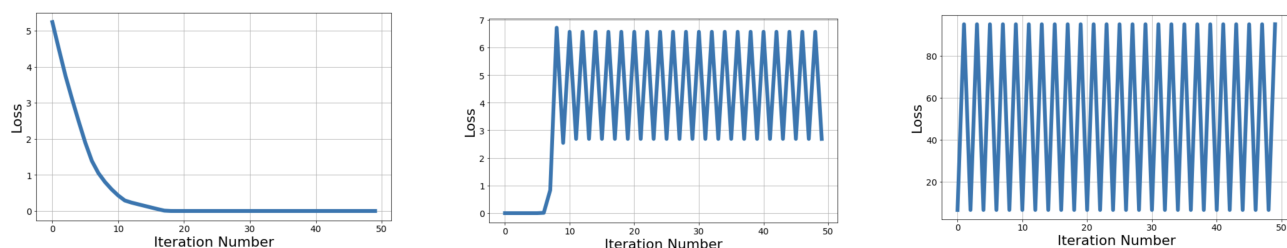


Figure 3. Training curves for  $\alpha = 0.1$ ,  $\alpha = 1$ , and  $\alpha = 10$  with the Lipschitz continuous Huber loss function. As the learning rate increases, the loss starts oscillating with larger frequencies, but never diverges to  $\infty$ . This is to be expected from Proposition 4.1, since the Huber loss function is convex, non-smooth and has bounded subgradients.

## References

- Ahn, K., Bubeck, S., Chewi, S., Lee, Y. T., Suarez, F., and Zhang, Y. Learning threshold neurons via the” edge of stability”. *arXiv preprint arXiv:2212.07469*, 2022a.
- Ahn, K., Zhang, J., and Sra, S. Understanding the unstable convergence of gradient descent. In *International Conference on Machine Learning*, pp. 247–257. PMLR, 2022b.
- Ahn, K., Bubeck, S., Chewi, S., Lee, Y. T., Suarez, F., and Zhang, Y. Learning threshold neurons via edge of stability. *Advances in Neural Information Processing Systems*, 36, 2024.
- Arora, S., Li, Z., and Panigrahi, A. Understanding gradient descent on the edge of stability in deep learning. In *International Conference on Machine Learning*, pp. 948–1024. PMLR, 2022.
- Bengio, Y. Practical recommendations for gradient-based training of deep architectures. *Neural Networks: Tricks of the Trade: Second Edition*, pp. 437–478, 2012.
- Bertoin, D., Bolte, J., Gerchinovitz, S., and Pauwels, E. Numerical influence of  $\text{relu}'(0)$  on backpropagation. *Advances in Neural Information Processing Systems*, 34: 468–479, 2021.
- Bertsekas, D. P. Nonlinear programming. *Journal of the Operational Research Society*, 48, 1997.
- Blalock, D., Gonzalez Ortiz, J. J., Frankle, J., and Gutttag, J. What is the state of neural network pruning? *Proceedings of machine learning and systems*, 2:129–146, 2020.
- Bolte, J. and Pauwels, E. Conservative set valued fields, automatic differentiation, stochastic gradient methods and deep learning. *Mathematical Programming*, 188:19–51, 2021.
- Bottou, L. Large-scale machine learning with stochastic gradient descent. In *Proceedings of COMPSTAT'2010: 19th International Conference on Computational Statistics Paris France, August 22-27, 2010 Keynote, Invited and Contributed Papers*, pp. 177–186. Springer, 2010.
- Bottou, L., Curtis, F. E., and Nocedal, J. Optimization methods for large-scale machine learning. *SIAM review*, 60(2):223–311, 2018.
- Boyd, S., Xiao, L., and Mutapcic, A. Subgradient methods. *lecture notes of EE392o, Stanford University, Autumn Quarter*, 2004:2004–2005, 2003.
- Boyd, S., Boyd, S. P., and Vandenberghe, L. *Convex optimization*. Cambridge university press, 2004.
- Chen, L. and Bruna, J. On gradient descent convergence beyond the edge of stability. *arXiv preprint arXiv:2206.04172*, 2022.
- Chen, Y., Ma, Z., Fang, W., Zheng, X., Yu, Z., and Tian, Y. A unified framework for soft threshold pruning. *arXiv preprint arXiv:2302.13019*, 2023.
- Cohen, J. M., Kaur, S., Li, Y., Kolter, J. Z., and Talwalkar, A. Gradient descent on neural networks typically occurs at the edge of stability. *arXiv preprint arXiv:2103.00065*, 2021.
- Dauphin, Y. N., Pascanu, R., Gulcehre, C., Cho, K., Ganguli, S., and Bengio, Y. Identifying and attacking the saddle point problem in high-dimensional non-convex optimization. *Advances in neural information processing systems*, 27, 2014.
- Davis, D., Drusvyatskiy, D., Kakade, S., and Lee, J. D. Stochastic subgradient method converges on tame functions. *Foundations of computational mathematics*, 20(1): 119–154, 2020.
- Défossez, A., Bottou, L., Bach, F., and Usunier, N. A simple convergence proof of adam and adagrad. *arXiv preprint arXiv:2003.02395*, 2020.

- Duchi, J., Hazan, E., and Singer, Y. Adaptive subgradient methods for online learning and stochastic optimization. *Journal of machine learning research*, 12(7), 2011.
- Efron, B., Hastie, T., Johnstone, I., and Tibshirani, R. Least angle regression. 2004.
- Friedman, J., Hastie, T., and Tibshirani, R. Sparse inverse covariance estimation with the graphical lasso. *Biostatistics*, 9(3):432–441, 2008.
- Friedman, J., Hastie, T., Tibshirani, R., Narasimhan, B., Tay, K., Simon, N., and Qian, J. Package ‘glmnet’. *CRAN R Repository*, 595, 2021.
- Ghosh, P., Azam, S., Jonkman, M., Karim, A., Shamrat, F. J. M., Ignatious, E., Shultana, S., Beeravolu, A. R., and De Boer, F. Efficient prediction of cardiovascular disease using machine learning algorithms with relief and lasso feature selection techniques. *IEEE Access*, 9: 19304–19326, 2021.
- Girshick, R. Fast r-cnn. In *Proceedings of the IEEE international conference on computer vision*, pp. 1440–1448, 2015.
- Goodfellow, I., Bengio, Y., and Courville, A. *Deep learning*. MIT press, 2016a.
- Goodfellow, I., Bengio, Y., and Courville, A. Regularization for deep learning. *Deep learning*, pp. 216–261, 2016b.
- Han, S., Mao, H., and Dally, W. J. Deep compression: Compressing deep neural networks with pruning, trained quantization and huffman coding. *arXiv preprint arXiv:1510.00149*, 2015a.
- Han, S., Pool, J., Tran, J., and Dally, W. Learning both weights and connections for efficient neural network. *Advances in neural information processing systems*, 28, 2015b.
- Hendrycks, D. and Gimpel, K. Gaussian error linear units (gelus). *arXiv preprint arXiv:1606.08415*, 2016.
- Ioffe, S. and Szegedy, C. Batch normalization: Accelerating deep network training by reducing internal covariate shift. In *International conference on machine learning*, pp. 448–456. pmlr, 2015.
- Kingma, D. P. and Ba, J. Adam: A method for stochastic optimization. *arXiv preprint arXiv:1412.6980*, 2014.
- Kramer, O. and Kramer, O. Scikit-learn. *Machine learning for evolution strategies*, pp. 45–53, 2016.
- Kumar, S. K. Analytical solutions for a family of single layer neural network regression problems, 2023. URL [https://openreview.net/forum?id=g6ZFp73\\_T7](https://openreview.net/forum?id=g6ZFp73_T7).
- Laurent, T. and Brecht, J. The multilinear structure of relu networks. In *International conference on machine learning*, pp. 2908–2916. PMLR, 2018.
- Le, Q. V., Ngiam, J., Coates, A., Lahiri, A., Prochnow, B., and Ng, A. Y. On optimization methods for deep learning. In *Proceedings of the 28th international conference on machine learning*, pp. 265–272, 2011.
- Li, H., Kadav, A., Durdanovic, I., Samet, H., and Graf, H. P. Pruning filters for efficient convnets. *arXiv preprint arXiv:1608.08710*, 2016.
- Li, J., Das, K., Fu, G., Li, R., and Wu, R. The bayesian lasso for genome-wide association studies. *Bioinformatics*, 27(4):516–523, 2011.
- Li, Z. and Sillanpää, M. J. Overview of lasso-related penalized regression methods for quantitative trait mapping and genomic selection. *Theoretical and applied genetics*, 125:419–435, 2012.
- Li, Z., Wang, Z., and Li, J. Analyzing sharpness along gd trajectory: Progressive sharpening and edge of stability. *arXiv preprint arXiv:2207.12678*, 2022.
- Liu, W., Anguelov, D., Erhan, D., Szegedy, C., Reed, S., Fu, C.-Y., and Berg, A. C. Ssd: Single shot multibox detector. In *Computer Vision—ECCV 2016: 14th European Conference, Amsterdam, The Netherlands, October 11–14, 2016, Proceedings, Part I 14*, pp. 21–37. Springer, 2016.
- Lydia, A. and Francis, S. Adagrad—an optimizer for stochastic gradient descent. *Int. J. Inf. Comput. Sci*, 6(5): 566–568, 2019.
- Ma, C., Wu, L., and Ying, L. The multiscale structure of neural network loss functions: The effect on optimization and origin. *arXiv preprint arXiv:2204.11326*, 2022.
- Ma, R., Miao, J., Niu, L., and Zhang, P. Transformed l1 regularization for learning sparse deep neural networks. *Neural Networks*, 119:286–298, 2019.
- Mazumder, R. and Hastie, T. The graphical lasso: New insights and alternatives. *Electronic journal of statistics*, 6:2125, 2012.
- McMahan, H. B. and Streeter, M. Adaptive bound optimization for online convex optimization. *arXiv preprint arXiv:1002.4908*, 2010.
- Ogutu, J. O., Schulz-Streeck, T., and Piepho, H.-P. Genomic selection using regularized linear regression models: ridge regression, lasso, elastic net and their extensions. In *BMC proceedings*, volume 6, pp. 1–6. Springer, 2012.

- Paszke, A., Gross, S., Chintala, S., Chanan, G., Yang, E., DeVito, Z., Lin, Z., Desmaison, A., Antiga, L., and Lerer, A. Automatic differentiation in pytorch. 2017.
- Reddi, S. J., Kale, S., and Kumar, S. On the convergence of adam and beyond. *arXiv preprint arXiv:1904.09237*, 2019.
- Ren, S., He, K., Girshick, R., and Sun, J. Faster r-cnn: Towards real-time object detection with region proposal networks. *Advances in neural information processing systems*, 28, 2015.
- Ruder, S. An overview of gradient descent optimization algorithms. *arXiv preprint arXiv:1609.04747*, 2016.
- Scardapane, S., Comminiello, D., Hussain, A., and Uncini, A. Group sparse regularization for deep neural networks. *Neurocomputing*, 241:81–89, 2017.
- Shi, N. and Li, D. Rmsprop converges with proper hyperparameter. In *International conference on learning representation*, 2021.
- Shor, N. Z. *Minimization methods for non-differentiable functions*, volume 3. Springer Science & Business Media, 2012.
- Siegel, J. W., Chen, J., Zhang, P., and Xu, J. Training sparse neural networks using compressed sensing. *arXiv preprint arXiv:2008.09661*, 2020.
- Simonyan, K. and Zisserman, A. Very deep convolutional networks for large-scale image recognition. *arXiv preprint arXiv:1409.1556*, 2014.
- Stevens, E., Antiga, L., and Viehmann, T. *Deep learning with PyTorch*. Manning Publications, 2020.
- Tibshirani, R. Regression shrinkage and selection via the lasso. *Journal of the Royal Statistical Society: Series B (Methodological)*, 58(1):267–288, 1996.
- Tibshirani, R. Subgradient method. In *Lecture Notes 10-725/36-725: Convex Optimization; Lecture 7*. 2015. URL <https://www.stat.cmu.edu/~ryantibs/convexopt-S15/scribes/07-sg-method-scribed.pdf>.
- Tibshirani, R., Saunders, M., Rosset, S., Zhu, J., and Knight, K. Sparsity and smoothness via the fused lasso. *Journal of the Royal Statistical Society: Series B (Statistical Methodology)*, 67(1):91–108, 2005.
- Tieleman, T., Hinton, G., et al. Lecture 6.5-rmsprop: Divide the gradient by a running average of its recent magnitude. *COURSERA: Neural networks for machine learning*, 4(2):26–31, 2012.
- Vaswani, A., Shazeer, N., Parmar, N., Uszkoreit, J., Jones, L., Gomez, A. N., Kaiser, Ł., and Polosukhin, I. Attention is all you need. *Advances in neural information processing systems*, 30, 2017.
- Wen, W., Wu, C., Wang, Y., Chen, Y., and Li, H. Learning structured sparsity in deep neural networks. *Advances in neural information processing systems*, 29, 2016.
- Xiao, L. Dual averaging method for regularized stochastic learning and online optimization. *Advances in Neural Information Processing Systems*, 22, 2009.
- Xiao, X., Wang, Z., and Rajasekaran, S. Autoprune: Automatic network pruning by regularizing auxiliary parameters. *Advances in neural information processing systems*, 32, 2019.
- Yang, C., Yang, Z., Khattak, A. M., Yang, L., Zhang, W., Gao, W., and Wang, M. Structured pruning of convolutional neural networks via l1 regularization. *IEEE Access*, 7:106385–106394, 2019.
- You, Y., Li, J., Reddi, S., Hseu, J., Kumar, S., Bhojanapalli, S., Song, X., Demmel, J., Keutzer, K., and Hsieh, C.-J. Large batch optimization for deep learning: Training bert in 76 minutes. *arXiv preprint arXiv:1904.00962*, 2019.
- Zhang, Y., Chen, C., Shi, N., Sun, R., and Luo, Z.-Q. Adam can converge without any modification on update rules. *Advances in Neural Information Processing Systems*, 35: 28386–28399, 2022.
- Zhang, Z. Improved adam optimizer for deep neural networks. In *2018 IEEE/ACM 26th international symposium on quality of service (IWQoS)*, pp. 1–2. Ieee, 2018.
- Zou, H. and Hastie, T. Regularization and variable selection via the elastic net. *Journal of the royal statistical society: series B (statistical methodology)*, 67(2):301–320, 2005.

## A. Appendix A - Architecture and code for Figure 2

The code to construct our plots in Figure 2, was taken from <https://github.com/kuangliu/pytorch-cifar/blob/master/models/vgg.py>, with three minor modifications. First, we removed the batch normalization as part of each layer. We did this because, while it is known that batch normalization alters the training dynamics (Ioffe & Szegedy, 2015), and our work is interested in the effect of network smoothness on convergence speed in the absence of confounders. Second, we replaced max pool with average pool to ensure differentiability of the layer, and third, we used a simpler layer configuration than one provided in the link. The configuration we used is provided below:

```
cfg = {
    'VGG11': [16, 'M', 32, 'M', 32, 32, 'M', 64, 64, 'M', 64, 64, 'M'],
    'VGG13': [16, 16, 'M', 32, 32, 'M', 32, 32, 'M', 64, 64, 'M', 64, 64, 'M'],
    'VGG19': [16, 16, 'M', 32, 32, 'M',
              32, 32, 32, 32, 'M',
              64, 64, 64, 64, 'M',
              64, 64, 64, 64, 'M'],
}
```

## B. Proof of proposition 3.1

Proposition 3.1 follows from the two propositions described below.

**Proposition B.1.** *Let  $\{\beta_t\}_{t=0}^\infty$  denote the sequence generated by running NDGM on (7), with a constant learning rate,  $\alpha$ , and the entries in  $\beta_0$  being uniformly sampled from  $[-1, 1]$ . Then  $\beta_k$  will have all non-zero entries with probability 1 for all  $k > 0$ .*

*Proof.* The NDGM iteration for (7) is described by the recursion

$$\beta_i[k] = \begin{cases} \beta_{i-1}[k] - \alpha\lambda_1 & \text{if } \beta_{i-1}[k] > 0 \\ \beta_{i-1}[k] + \alpha\lambda_1 & \text{if } \beta_{i-1}[k] < 0 \\ 0 & \text{if } \beta_{i-1}[k] = 0 \end{cases} \quad (11)$$

From (11), it is clear that if the  $k^{\text{th}}$  entry in the vector becomes zero during any iteration, then it stays zero for all subsequent iterations. Accordingly, suppose the  $k^{\text{th}}$  entry in the NDGM sequence vector becomes 0 for the first time after  $N$  iterations. Then we have

$$\beta_N[k] = \beta_0[k] + (N - 2m)\alpha\lambda_1 = 0, \quad (12)$$

where  $m$  is the number of times the  $k^{\text{th}}$  entry of the parameter exceeds 0 in the first  $N$  iterations. (12) can only hold if  $\beta_0[k]$ , is an integer multiple of  $\alpha\lambda_1$ . Since the feasible values are countable, and the set of initializations is uncountable, the probability of the occurrence has measure 0.  $\square$

In the next proposition, we show that the sequence does not converge, but oscillates between two fixed points.

**Proposition B.2.** *The sequence  $\{\beta_t\}_{t=0}^\infty$  described in the previous proposition does not converge. Furthermore, there exists an integer  $N_0$ , such that for every  $N \geq N_0$ , we can write*

$$\beta_{n_k+m}[k] = \begin{cases} \gamma_k - \alpha\lambda_1 & \text{if } m \text{ is odd} \\ \gamma_k & \text{if } m \text{ is even,} \end{cases} \quad (13)$$

for some  $\gamma_k \in (0, \alpha\lambda_1)$  for all  $0 \leq k \leq P - 1$ .

*Proof.* We prove the results assuming  $\beta_0[k] > 0$ ; the proof is similar when  $\beta_0[k] < 0$ . From Proposition B.1, we know that for any  $N > 0$ ,  $\beta_N[k] \neq 0$  with probability 1. Therefore, (11) implies that starting from any  $\beta_0[k] > 0$ , the sequence will

decrease monotonically till it reaches a value between 0 and  $\alpha\lambda_1$ . Accordingly, let  $\beta_{n_k}[k] = \gamma_k$  for some  $n_k \geq 0$ , with  $\gamma_k \in (0, \alpha\lambda_1)$ . Since  $\gamma_k - \alpha\lambda_1 < 0$ , completing the recursion in (11) gives

$$\beta_{n_k+m}[k] = \begin{cases} \gamma_k - \alpha\lambda_1 & \text{if } m \text{ is odd} \\ \gamma_k & \text{if } m \text{ is even.} \end{cases} \quad (14)$$

The result follows by choosing  $N_0 = \max(n_0, n_1 \dots n_{P-1})$ . □

### C. NDGM unreliability for the general LASSO problem

In this section, we demonstrate via simulations that the problems demonstrated in our toy LASSO problem hold even for the general setting. Consider the loss function for the general LASSO problem given by

$$L_4(\beta; \mathbf{W}, \mathbf{y}, \lambda_1) = \frac{1}{N} \|\mathbf{y} - \mathbf{W}\beta\|_2^2 + \lambda_1 \|\beta\|_1, \quad (15)$$

where  $\mathbf{W}$  is an arbitrary  $20 \times 500$  dimensional data matrix, and  $\mathbf{y}$  is an arbitrary  $20 \times 1$  response, each of whose entries are sampled from the uniform distribution on  $[-1, 1]$ . We run NDGM on (15) twice with the same learning rate and initialization, once with  $\lambda_1 = 0.01$ , and once with  $\lambda_1 = 10$ . At the end of the two runs, the optimal solution with  $\lambda_1 = 0.1$  has an  $L_1$  norm of 1.62, and the optimal solution with  $\lambda_1 = 10$  has an  $L_1$  norm of 25.4 i.e., a 1000 fold increase in the value of  $\lambda_1$  results in a more than 15 fold increase in the  $L_1$  norm of the optimal solution!

### D. Different NGDM variants and the LASSO

In this section, we demonstrate that various NDGM variants, traditionally thought to converge similarly based on the analysis of differentiable functions, exhibit notably distinct behaviors even when applied to the simple non-differentiable toy LASSO problem outlined in (7). A summary of our findings are in Table D.

NDGM variant	Unique characteristic
Vanilla NDGM (including SGD)	$\beta_0$ and $\lambda_1$ influence eventual values of the sequence. If sequence hits 0, then stays 0.
NDGM with momentum	If sequence hits 0, then jumps away from 0.
RMSProp	Only $\beta_0$ influences the eventual value of the sequence. If sequence hits 0, then stays 0.

#### D.1. SGD and the LASSO

Since the gradient of (7) is independent of the batch in question, the results in Proposition B.2 hold for the SGD case as well.

#### D.2. NDGM with momentum and the LASSO

With the vanilla NDGM, (11) gives the guarantee that once a parameter value reaches zero during an iteration, it remains zero in all future iterations. We show that NDGM with momentum does not provide this guarantee.

**Proposition D.1.** *Let  $\{\beta_t\}_{t=0}^\infty$  denote the sequence generated by running NDGM with momentum on (7), with a constant learning rate,  $\alpha$ , and the entries in  $\beta_0$  being uniformly sampled from  $[-1, 1]$ . Suppose  $\beta_{N-1}[k] \neq 0$  and  $\beta_N[k] = 0$ , then  $\beta_{N+1}[k] \neq 0$ .*

*Proof.* With a momentum factor of  $\eta$ , NGDM with momentum can be written as (see page 6 of [https://www.ceremade.dauphine.fr/~waldspurger/tds/22\\_23\\_s1/advanced\\_gradient\\_descent.pdf](https://www.ceremade.dauphine.fr/~waldspurger/tds/22_23_s1/advanced_gradient_descent.pdf) for details)

$$\beta_{N+1}[k] = \beta_N[k] - \alpha(1 - \eta)\nabla L_3(\beta_N)[k] + \eta(\beta_N[k] - \beta_{N-1}[k]) \quad (16)$$

Since  $\beta_N[k] = 0$ , we have  $\nabla L_3(\beta_N)[k] = 0$ , and therefore,

$$\beta_{N+1}[k] = -\eta\beta_{N-1}[k] \neq 0, \quad (17)$$

hence the result. □

### D.3. RMSProp and the LASSO

Proposition B.2 shows that the vanilla NDGM sequence eventually bounces between two vectors which depend on the strength of regularization,  $\lambda_1$ , and the weight initialization,  $\beta_0$ . Here we show that RMSProp, which is a near scale invariant NDGM sequence bounces between two vectors whose orientation depends only on  $\beta_0$ . The RMSProp equations (equation 18 in (Ruder, 2016)) can be written as

$$v_t[k] = \gamma v_{t-1}[k] + (1 - \gamma) (\nabla L_3(\beta_N)[k])^2, \text{ and} \quad (18)$$

$$\beta_{t+1}[k] = \beta_t[k] - \frac{\alpha}{\sqrt{v_t[k] + \bar{\epsilon}}} \nabla L_3(\beta_t)[k], \quad (19)$$

where  $v_0[k] = 0$ ,  $\gamma$  is a scaling factor with a typical default value of 0.99, and  $\bar{\epsilon}$  is a small positive jitter added to prevent division by 0. If  $\beta_N[k] \neq 0$ , we have  $(\nabla L_3(\beta_N)[k])^2 = \lambda_1^2$ . Using this fact in (18), we note that  $v_1[k] = (1 - \gamma)\lambda_1^2$ , and  $v_2[k] = (1 - \gamma^2)\lambda_1^2$ . Completing the recursion we get

$$v_t[k] = (1 - \gamma^t)\lambda_1^2. \quad (20)$$

Plugging (20) into (19) with  $\epsilon = \bar{\epsilon}/\lambda_1^2$  gives

$$\beta_{t+1}[k] = \beta_t[k] - \frac{\alpha}{\sqrt{1 + \epsilon - \gamma^t}} \text{sign}(\beta_t[k]), \quad (21)$$

which we use as a base in our analysis. We now provide the key results for RMSProp:

**Proposition D.2.** *Let  $\{\beta_t\}_{t=0}^\infty$  denote the sequence generated by running the RMSProp recursion described in (21), with a constant learning rate,  $\alpha$ , and the entries in  $\beta_0$  being uniformly sampled from  $[-1, 1]$ . Then  $\beta_t$  will have all non-zero entries with probability 1 for all  $t > 0$ .*

Suppose the  $k^{\text{th}}$  entry in the RMSProp sequence vector becomes 0 for the first time after  $N$  iterations. Then, completing the recursion in (21) we have

$$\beta_N[k] = \beta_0[k] + \sum_{i \in Q} \frac{\alpha}{\sqrt{1 + \epsilon - \gamma^i}} - \sum_{j \in P} \frac{\alpha}{\sqrt{1 + \epsilon - \gamma^j}} = 0, \quad (22)$$

where  $Q$  is the set of all iteration numbers where the parameter value is less than 0 and  $P$  is the set of all iteration numbers where the parameter value is greater than 0, with  $|P| + |Q| = N$ . Let  $C(N)$  denote the set of all values of  $\beta_0[k]$  which satisfy (22). The cardinality of  $C(N)$  is at most equal to the number of ways of partitioning  $N$  integers into 2 sets,  $P$  and  $Q$ . Therefore,  $C(N)$  is countable, and the superset of all feasible values of  $\beta_0[k]$  which lead to a sparse solution given by  $\bigcup_{I=1}^\infty C(I)$  is countable. Since the initializations are uncountable, the probability of the event has measure 0.

**Proposition D.3.** *The RMSProp sequence described in (21) eventually behaves like a vanilla NGDM sequence with a LASSO penalty of 1 irrespective of the value of  $\lambda_1$  chosen in the original problem.*

*Proof.* From the previous proposition, we know that  $\beta_t[k] \neq 0$  with probability 1 even for large values of  $t$ . Furthermore, we note that even after a modest number of iterations the scaling term becomes negligible; for instance, with  $t = 1000$ ,  $\gamma^t = O(10^{-5})$ . Accordingly, assuming that in the large  $t$  limit we have  $\epsilon \ll \gamma^t \ll 1$ , we can use first order Taylor expansions to write

$$\beta_{t+1}[k] = \beta_t[k] - \alpha \text{sign}(\beta_t[k]) + O(\gamma^t), \quad (23)$$

which is the recursion for the vanilla NGDM algorithm with a LASSO penalty of 1 up to first order.  $\square$

## E. Connections to deep learning training theory:

The conventional wisdom in deep learning is that different NDGM variants converge at varying rates, but eventually reach similar near-optimal values by the end of training. In this section, we demonstrate problems with this assumption using our toy LASSO problem from Equation (7).

Since the vector of zeros is the unique global minimizer of Equation (7), we expect the vanilla NDGM and RMSProp sequences to converge to this value by the end of training. Accordingly, we anticipate the  $L_1$  norms of the sequences

generated using these two variants to converge to comparable near-zero values after training completes. Because the loss function in Equation (7) is the  $L_1$  norm of the weights scaled by a factor of  $\lambda_1$ , we expect the NDGM and RMSProp training curves to also hover around 0 at the end of training, exhibiting substantial overlap. To test this hypothesis, we ran vanilla NDGM and RMSProp on Equation (7) with identical initializations and learning rates, plotting the final 100 training iterations for each sequence using two different  $\lambda_1$  values. As Figure 4 shows, the two sequences display no overlap for either  $\lambda_1$  value. Moreover, the RMSProp solution consistently has a higher loss (and  $L_1$  norm) across all 100 iterations when  $\lambda_1 = 0.001$ , while vanilla NDGM always yields a higher value when  $\lambda_1 = 1$ . Conventional analysis of differentiable functions cannot explain this peculiarity, but our findings provide intuition into the underlying reasons. To explain these findings, we use the following proposition:

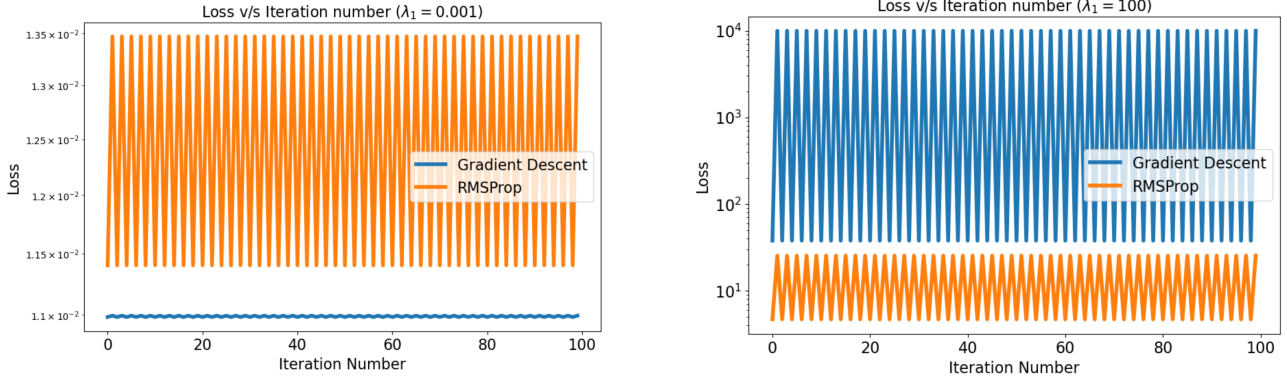


Figure 4. Comparison of the training curves of RMSProp and vanilla NDGM with  $\lambda_1 = 0.001$ , and  $\lambda_1 = 100$  for the toy LASSO problem considered in (7) with  $P = 10$  and  $\alpha = 0.1$ . We note that when  $\lambda_1 \ll 1$ , the RMSProp training curve lies above the vanilla NDGM training curve, and the reverse is true for  $\lambda_1 \gg 1$ .

**Proposition E.1.** For the vanilla NDGM sequence we have  $0 < \liminf_{N \rightarrow \infty} \|\beta_N\|_1 \leq \limsup_{N \rightarrow \infty} \|\beta_N\|_1 < P\alpha\lambda_1$ , where  $P$  is the number of rows in  $\beta_0$ .

*Proof.* From Proposition B.2, we note that  $\liminf_{N \rightarrow \infty} |\beta_N[k]| > 0$  and  $\limsup_{N \rightarrow \infty} |\beta_N[k]| < \alpha\lambda_1$  for all  $k$ . Therefore,  $0 < \sum_{i=0}^{P-1} \liminf_{N \rightarrow \infty} |\beta_N[i]| \leq \liminf_{N \rightarrow \infty} \|\beta_N\|_1 \leq \limsup_{N \rightarrow \infty} \|\beta_N\|_1 \leq \sum_{i=0}^{P-1} \limsup_{N \rightarrow \infty} |\beta_N[i]| < P\alpha\lambda_1$ .  $\square$

We know from propositions B.2 and D.3 that the vanilla NDGM sequence and the RMSProp sequence eventually bounce (approximately) between two points each. Let  $v_1(\beta_0, \lambda_1)$  and  $v_2(\beta_0, \lambda_1)$  indicate the points around which the vanilla NDGM sequence bounces, and let  $r_1(\beta_0, \lambda_1)$  and  $r_2(\beta_0, \lambda_1)$  indicate the points around which the RMSProp sequence bounces. From propositions E and B.2 we have that  $\min(\lambda_1\|v_1(\beta_0, \lambda_1)\|_1, \lambda_1\|v_2(\beta_0, \lambda_1)\|_1) < P\alpha\lambda_1^2$ , and  $\max(\lambda_1\|v_1(\beta_0, \lambda_1)\|_1, \lambda_1\|v_2(\beta_0, \lambda_1)\|_1) < P\alpha\lambda_1^2$ . From proposition D.3 we have that the RMSProp sequence eventually behaves like a vanilla NDGM sequence with a LASSO penalty of 1, and therefore, we have  $\min(\lambda_1\|r_1(\beta_0, \lambda_1)\|_1, \lambda_1\|r_2(\beta_0, \lambda_1)\|_1) < P\alpha\lambda_1$ , and  $\max(\lambda_1\|r_1(\beta_0, \lambda_1)\|_1, \lambda_1\|r_2(\beta_0, \lambda_1)\|_1) < P\alpha\lambda_1$ . Therefore, when  $\lambda_1 \ll 1$ , we intuitively expect  $\max(\lambda_1\|v_1(\beta_0, \lambda_1)\|_1, \lambda_1\|v_2(\beta_0, \lambda_1)\|_1) < \min(\lambda_1\|r_1(\beta_0, \lambda_1)\|_1, \lambda_1\|r_2(\beta_0, \lambda_1)\|_1)$ , and when  $\lambda_1 \gg 1$  we expect  $\max(\lambda_1\|r_1(\beta_0, \lambda_1)\|_1, \lambda_1\|r_2(\beta_0, \lambda_1)\|_1) < \min(\lambda_1\|v_1(\beta_0, \lambda_1)\|_1, \lambda_1\|v_2(\beta_0, \lambda_1)\|_1)$ , which is what the figure shows.

To clarify the ideas, suppose  $P = 10$  and  $\alpha = 0.1$ . The above propositions state that with  $\lambda_1 = 0.01$ , the RMSProp loss oscillates between two positive values, each less than 0.01, while the vanilla NDGM loss oscillates between two positive values, each less than 0.0001. Consequently, when  $\lambda_1$  is significantly less than 1, it is reasonable to anticipate the RMSProp loss will typically be greater than the vanilla NDGM loss at training's end. However, when  $\lambda_1 = 100$ , the RMSProp loss oscillates between two positive values under 100, whereas the vanilla NDGM loss oscillates between two values under 10,000. Accordingly, when  $\lambda_1$  is significantly greater than 1, the RMSProp loss is expected to be less than the vanilla NDGM loss in most scenarios at training's conclusion, as demonstrated in the figure.

## F. Experiments with the LASSO penalty:

In this section, we provide the graphs and tables resulting from the experiments outlined in Section 3, along with the respective code to generate them.

### F.1. $L_1$ norm v/s iteration number using different NDGM variants

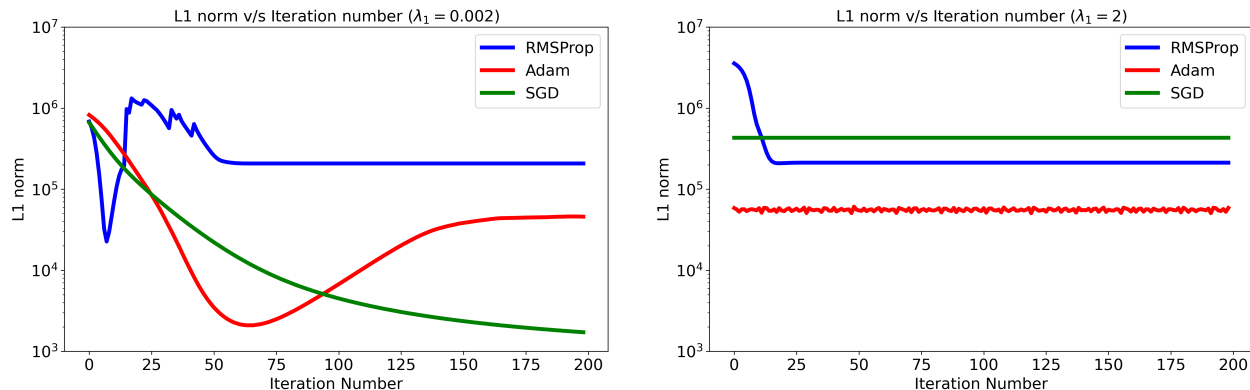


Figure 5. Comparison of the training curves of RMSProp, SGD and Adam for a pretrained VGG16 finetuned using the  $L_1$  penalized cross entropy loss. All 6 training runs are initialized with the same weights, use the same learning rate, and are fed in batches in the same sequence.

### F.2. Percentage of weights less than $10^{-5}$ for different NDGM variants

Variant	$\lambda_1 = 0.002$	$\lambda_1 = 2$
SGD	99.89%	0.18%
RMSProp	0.09%	1.21%
Adam	3.31%	2.28%

Table 1. A comparison of the percentage of weights having absolute value less than  $10^{-5}$  across the three NDGM variants. We note for Adam and SGD that increasing the  $L_1$  norm can lead to a reduction in the percentage of prunable parameters.

### F.3. Code for generating the above plots (GPT generated and validated for correctness)

```
import torch
import torch.nn as nn
import torch.optim as optim
from torchvision import datasets, transforms, models
import copy

# Set random seed for reproducibility
seed = 42
torch.manual_seed(seed)
torch.backends.cudnn.deterministic = True
torch.backends.cudnn.benchmark = False
import numpy as np
np.random.seed(seed)

# Set device to GPU if available
device = torch.device("cuda" if torch.cuda.is_available() else "cpu")
```

```
# Define transform and download CIFAR-10 dataset
transform = transforms.Compose([
    transforms.ToTensor(),
    transforms.Normalize((0.5, 0.5, 0.5), (0.5, 0.5, 0.5)),
])

train_dataset = datasets.CIFAR10(root='./data',
                                 train=True,
                                 download=True,
                                 transform=transform)
train_loader = torch.utils.data.DataLoader(train_dataset,
                                           batch_size=512,
                                           shuffle=False,
                                           num_workers=4)

test_dataset = datasets.CIFAR10(root='./data',
                                 train=False,
                                 download=True,
                                 transform=transform)
test_loader = torch.utils.data.DataLoader(test_dataset,
                                          batch_size=128,
                                          shuffle=False,
                                          num_workers=2)

def compute_validation_loss(net):
    val_loss = 0.0
    total = 0
    with torch.no_grad():
        for data in test_loader:
            images, labels = data
            images, labels = images.to(device), labels.to(device)
            outputs = net(images)
            loss = criterion(outputs, labels)
            val_loss += loss.item()
            total += labels.size(0)
    return val_loss / total

def train(model, optimizer, l1_strength, num_epochs):
    train_losses, val_losses, l1_norms = [], [], []
    for epoch in range(num_epochs):
        epoch_loss = 0
        for inputs, labels in train_loader:
            inputs, labels = inputs.to(device), labels.to(device)

            # Forward pass
            outputs = model(inputs)
            loss_ce = criterion(outputs, labels)

            # L1 penalty
            l1_penalty = 0
```

## GD doesn't make the cut

---

```
for param in model.parameters():
    l1_penalty += torch.abs(param).sum()

# Add L1 penalty to the loss
loss = loss_ce + l1_strength * l1_penalty

# Backward and optimize
optimizer.zero_grad()
loss.backward()
optimizer.step()
epoch_loss += loss.item()
l1_norms.append(l1_penalty.item())
train_losses.append(epoch_loss / len(train_loader))
val_losses.append(compute_validation_loss(model))
print(f"Epoch: {epoch}, loss: {train_losses[-1]}, val loss: {val_losses[-1]}")
return train_losses, val_losses, l1_norms

# Model initialization
vgg16 = models.vgg16(pretrained=True)
initial_state = copy.deepcopy(vgg16.state_dict())
vgg16.to(device)

optimizers = {
    'SGD': optim.SGD(vgg16.parameters(), lr=0.003),
    'RMSProp': optim.RMSprop(vgg16.parameters(), lr=0.003),
    'Adam': optim.Adam(vgg16.parameters(), lr=0.003)
}

def get_num_prunable_params(model, threshold = 1e-5):
    total_params, num_small_params = 0, 0
    for name, param in model.named_parameters():
        total_params += param.numel()
        if 'weight' in name or 'bias' in name:
            num_small_params += torch.sum(torch.abs(param) < threshold).item()

    return num_small_params / total_params

loss_curves = {}
l1_norms_curves = {}
validation_loss_curves = {}
num_prunable_params = {}
for name, opt in optimizers.items():
    loss_curves[name],
    validation_loss_curves[name],
    l1_norms_curves[name],
    num_prunable_params[name] = {}, {}, {}, {}
for lambda1 in [2, 0.002]:
    print(f"opt: {name}, lambda: {lambda1}")
    vgg16.load_state_dict(copy.deepcopy(initial_state)) # Reset model
    losses, validation_losses, l1_norms = train(vgg16, opt, lambda1, 200)
```

## GD doesn't make the cut

---

```
num_prunable_params[name][lambda1] = get_num_prunable_params(vgg16)
loss_curves[name][lambda1] = losses
validation_loss_curves[name][lambda1] = validation_losses
l1_norms_curves[name][lambda1] = l1_norms
```